

Energetic electrons in impulsive solar flares: Radio diagnostics

Karl-Ludwig Klein

Observatoire de Paris, LESIA, CNRS-UMR 8109, 92195 Meudon, France

Received 2 November 2004; received in revised form 22 February 2005; accepted 11 March 2005

Abstract

Radio emissions during and outside solar flares are tracers of energetic electrons from the bottom of the corona to the interplanetary space. This review focusses on impulsive flares, where joint analyses of radio, hard X-ray and γ -ray observations proved to be powerful probes of the properties of accelerated electrons and of the sites in the corona where they are accelerated. Evidence of electron acceleration and transport in the corona from microwave imaging and decimetre wave spectroscopy is reviewed and compared, and recent work on the interpretation of microwave spectra in terms of energetic electron spectra is discussed. The two directions for future instrumentation are the extension to shorter wavelengths, with the aim of probing relativistic electrons, and solar dedicated spectral imaging from centimetric to metric waves to provide a unified view of the acceleration signatures that stem so far from different instruments with either spectroscopic or imaging capabilities.

© 2005 COSPAR. Published by Elsevier Ltd. All rights reserved.

Keywords: Sun: particle acceleration; Sun: flares; Sun: radio emission; Sun: Hard X-rays, γ -rays

1. Introduction

Radio emission of solar flares ranges from microwaves (wavelengths $\lesssim 30$ cm, corresponding to frequencies $\gtrsim 1$ GHz) emitted in the low corona to kilometre wavelengths (some tens of kHz) close to the Earth. The emission is invariably due to energetic, nearly always non-thermal, electron populations.

The following review will focus on the microwave emission from impulsive flares. In this domain, a large amount of new imaging and spectroscopic observations has become available and will be most useful in collaborative efforts with RHESSI. Section 2 will discuss microwave imaging and spectral observations and their joint analysis with hard X-rays (HXR) to extract information on the radiating electrons. At decimetric and metric wavelengths, a rich variety of spectral signatures is observed which gives information on the regions of electron acceleration. Because these emissions are coher-

ent, they are sensitive tracers of energetic electrons in regions of the corona that are too tenuous to provide detectable X-ray or γ -ray signatures. An overview of recent observations and their comparison with microwave analyses is attempted in Section 3. More detailed discussions of radio, X-ray and γ -ray diagnostics of particle acceleration during flares can be found in [Aschwanden \(2002\)](#) and [Vilmer and MacKinnon \(2003\)](#).

2. Microwave emission of solar flares

2.1. Morphology of simple microwave sources

Most microwave emission is produced through the (incoherent) gyrosynchrotron process. The mechanism is well understood (see, e.g., the review of [Dulk, 1985](#)) and can be used as a complementary diagnostic of the energy spectra of flare-accelerated electrons at energies $\gtrsim 100$ keV. Two major differences are to be noticed with respect to hard X-rays: besides on the radiating elec-

E-mail address: ludwig.klein@obspm.fr

trons, gyrosynchrotron emission depends also sensitively on the direction and strength of the ambient magnetic field, and the emission may be subject to absorption processes, including self-absorption by the energetic electrons and absorption by the ambient electrons at cm-to-mm wavelengths through free-free transitions.

Microwave source morphologies have been observed with spatial resolution of $10''$ or better by the *Very Large Array* (VLA), the *Siberian Solar Radio Telescope* (SSRT) and the *Nobeyama Radioheliograph* (NoRH). Many early observations of the VLA, using its extended configuration with the highest resolving power, probably missed part of the flare and may not have traced the relevant source configurations (Kai, 1987). Fig. 1 illustrates two more recent observations of simple source configurations: in (a), two-frequency observations (VLA) are shown on top of a magnetogram. The source at low frequencies (5 GHz, solid contours) is extended and bridges a line where the line-of-sight component of the photospheric magnetic field changes direction. At high frequencies (15 GHz, dashed contours) two smaller sources are observed on different sides of the large source at low frequencies. This configuration corresponds to the expectation of gyrosynchrotron models from magnetic loop configurations, for which detailed numerical models can be found in Alissandrakis and Preka-Papadema (1984), Preka-Papadema and Alissandrakis (1988, 1992) and Klein and Trotter (1984). At low frequencies the source is optically thick (self-absorption). Only the outer layers are seen, which means in this case the whole loop system or an extended region around its summit. With increasing frequency one distinguishes more and more clearly the two legs or footpoints, since the optically thin gyrosynchrotron intensity increases strongly with the magnetic field strength (power $0.90\delta - 1.22$ in the mildly relativistic case, where δ is the power-law spectral index of the radiating electrons; Dulk and Marsh, 1982). Therefore, radio imaging at frequencies below the spectral peak gives an impression of the overall source structure, while imaging above the peak frequency singles out the regions of strongest magnetic field. A qualitative discussion of gyrosynchrotron source morphologies and spectra in a dipolar configuration is given in Bastian et al. (1998). Circular polarisation can reveal further details of the source configuration. But it is subject to modification during the propagation of the radiation and cannot be reliably interpreted without detailed independent knowledge of the magnetic field structure in the corona.

Not all radio sources are resolved with the contemporary instrumentation. The total intensity map of the *Nobeyama Radioheliograph* in Fig. 1(b) shows a simple source overlying the line of magnetic field reversal. More structured patterns in the polarisation image (not

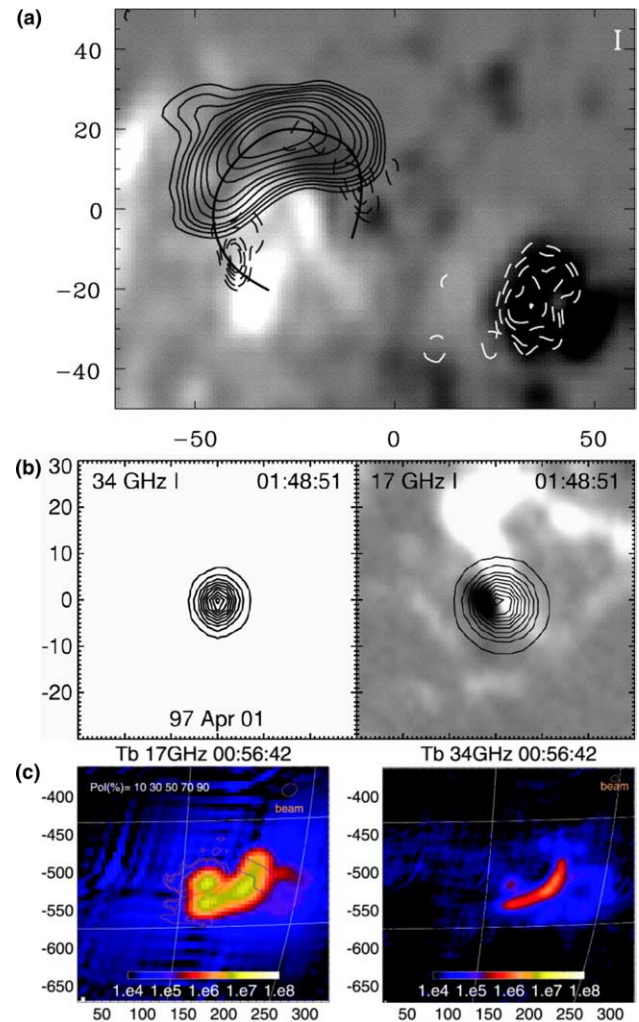


Fig. 1. Maps of microwave sources during flares. (a) Extended source (loop) at 5 GHz (solid contours), with two sources on either side at 15 GHz (dashed lines), VLA, on top of a line-of-sight magnetogram (Nindos et al., 2000). (b) Compact source at 34 GHz (left) and 17 GHz (right), NoRH, on top of a magnetogram (Kundu et al., 2001). (c) Extended loop-like structure at 17 GHz (left) and 34 GHz, NoRH (Yokoyama et al., 2002). The colour bar indicates brightness temperature. The axes are graded in arcseconds. (For interpretation of the references to colour in this figure legend, the reader is referred to the web version of this article.)

shown) suggest that the apparently compact source is actually unresolved.

Once the correspondence between simple models and simple observed configurations has been highlighted, it is instructive to look for counterexamples. Yokoyama et al. (2002) observed a simple elongated structure at two frequencies that they interpret as a loop filled with energetic electrons (Fig. 1(c)). The structure looks globally similar at 17 and 34 GHz, although the emission is optically thin at 34 GHz, where footpoint sources would therefore have been expected from the above arguments. It seems that the simple gyrosynchrotron models do not explain each observation, which may be due to

unresolved fine structure, complex particle dynamics in loops, or non-isotropic electron distributions. These issues will be touched upon again in Section 2.5.

2.2. Microwave sources and the evolution of coronal structures during flares

Hanaoka (1997) and Nishio et al. (1997) presented surveys of radio source morphologies observed by NoRH during events with simple time profiles at 17 GHz which are similar to HXR, and compared them with X-ray images (Fig. 2). They reported double (or multiple) loops during most events, one loop being compact ($\leq 20''$) and coinciding with a double HXR source, and a second loop on larger spatial scale ($30''$ – $80''$), with radio emission near the footpoint remote from the primary loop. The “loop” structure was identified by comparison with soft X-ray images. The compact microwave sources have internal structure, because the images in polarisation are not identical to those in total intensity. The brightness of the remote source varied in correlation with the primary one. Hanaoka (1999) made a correlation analysis between the microwave and HXR emissions in this type of source. He showed that the 17 GHz emission from the primary source co-evolved with the HXR emission (delay 0–0.2 s), while the remote source was significantly delayed (0.40–0.55 s). The configuration was interpreted as a signature of reconnection between a small emerging loop, which hosts the HXR

sources and the primary microwave source, and an overlying large scale loop. Hanaoka (1999) suggested that electrons are accelerated at the interface between the small emerging loop and the large overlying one, are injected into both the compact and the large loop, and are seen in the latter when reaching the opposite footpoint. Given the size of the compact loop, the reconnection region would be expected at a height of about 10^4 km above the footpoints. The delays and distances involved imply a speed along the large loop corresponding to electrons with energies of several hundreds of keV. Yokoyama et al. (2002) suggest that they directly imaged the propagation of electrons in such a loop.

2.3. Microwave flux densities and spectra

After many years of patrol observations at a few discrete frequencies, the Owens Valley Solar Array (OVSA) is the first to provide a quasi-continuous coverage of the spectrum between 1 and 18 GHz. A typical spectrum out of a sample of 412 events studied by Nita et al. (2004) is plotted in Fig. 3(a): at frequencies above 3 GHz the spectrum has the shape expected for gyrosynchrotron emission, with a rise to a peak near 5 GHz and a decay towards higher frequencies. The emission below 3 GHz is different, probably mostly coherent emission typical of decimetric and longer waves. The scatter plot in Fig. 3(b) displays the flux density as a function of frequency measured at the spectral peak for all points during the

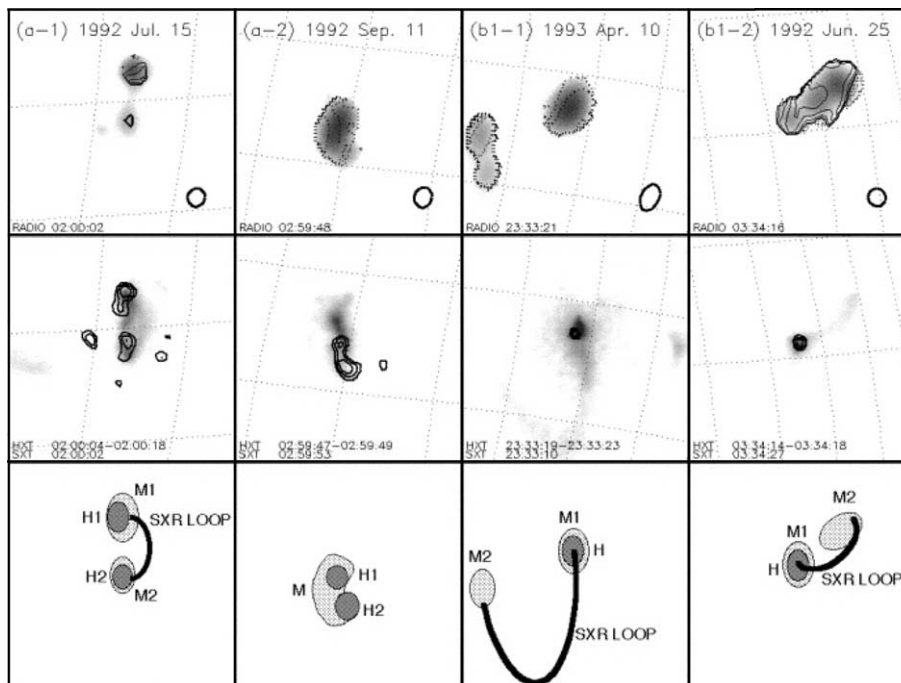


Fig. 2. Examples of source configurations observed by the NoRH (Nishio et al., 1997). Four events are shown in the four columns, the rows present maps at 17 GHz (top; NoRH) in intensity (grey-scale) and degree of circular polarisation (contours), HXR maps (middle; contours; Yokoh/HXT 23–33 keV) on top of a grey-scale soft X-ray image (Yokoh/SXT), a schematic drawing of the source configuration (bottom).

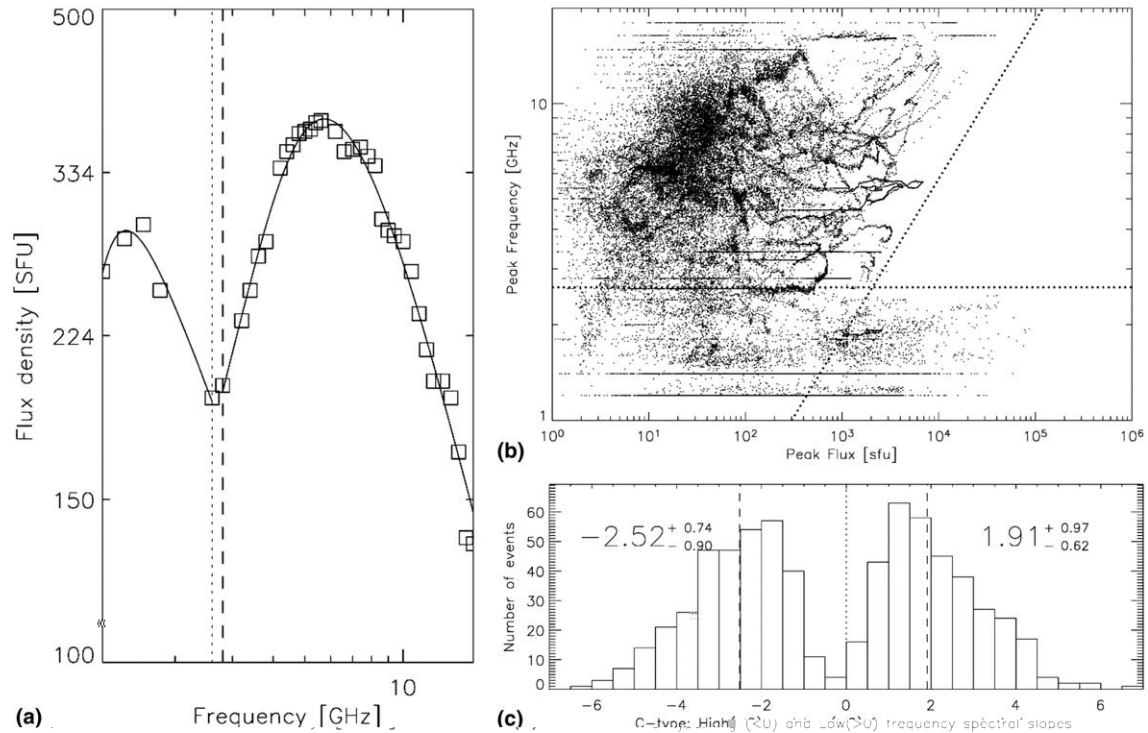


Fig. 3. Microwave spectrum and statistical parameters observed by the Owens Valley Solar Array (Nita et al., 2004). (a) An observed spectrum (open squares) with a simple analytical fit; the vertical dashed lines mark the limit between the high-frequency gyrosynchrotron spectrum and the domain of coherent emission at lower frequencies. (b) Scatter plot of measured peak flux densities vs. peak frequency throughout the events. (c) Histograms of the (positive) low-frequency and the (negative) high-frequency power-law indices of the observed spectra.

whole set of events. An important feature expected from gyrosynchrotron models is the correlation between the peak flux density and the frequency where it occurs, which is readily visible at frequencies above the dotted horizontal line. This means that the stronger the event, the higher its peak frequency, and the greater the probability that the emission is optically thick – or at least not optically thin – even at high frequencies. Based on an extensive statistical study (Guidice and Castelli, 1975), which showed that most microwave events had spectral maxima near 10 GHz, emission at higher frequencies was often implicitly assumed to be optically thin, and information was deduced on the electron number from single frequency observations. This is to be considered with much caution. Correia et al. (1994) had shown earlier, using 115 events observed with the whole Sun patrol observations of the University of Bern between 1984 and 1992, that nearly half of the bursts could not be considered as being optically thin in the range (20–35) GHz. This is not in contradiction with Guidice and Castelli (1975), but simply means that the bursts which are well observed at 35 GHz are relatively rare in their sample of microwave events. It is clear that multifrequency observations are required for any quantitative analysis of the microwave observations.

The low-frequency gyrosynchrotron spectrum may be shaped by self absorption by the non-thermal electrons,

by absorption in the ambient (thermal) plasma, or by suppression of gyrosynchrotron emission and absorption in a dense plasma at frequencies not too far from the electron plasma frequency (Razin suppression). Razin suppression generates a rather steep low-frequency spectrum. The distributions of observed spectral indices below (positive values) and above the spectral peak (negative values) are plotted in Fig. 3(c). A uniform gyrosynchrotron source containing an isotropic power-law distribution of electrons with spectral index δ (number of electrons $N(E)dE \sim E^{-\delta}dE$) produces an intensity spectrum with index $2.52 + 0.08\delta$ (cf. Dulk and Marsh, 1982) in the optically thick regime. A non-uniform magnetic field flattens the spectrum at low frequencies. OVSA (Fig. 3(c)) measures positive spectral indices with a median slightly flatter than 2. A significant number of spectra is steeper than 3 at low frequencies. This has generally been ascribed to Razin suppression in a dense ambient plasma (Ramaty, 1969; Klein, 1987; Belkora, 1997) or to the thermal absorption of emission from non-thermal electrons (Benka and Holman, 1992).

The high-frequency spectral slope of gyrosynchrotron emission reflects the slope of the electron spectrum (for isotropic electron distributions). The spectral index of the microwave intensity or flux density ($\sim \nu^\alpha$) predicted by simple homogeneous gyrosynchrotron models (Dulk and Marsh, 1982) is $\alpha = 1.22 - 0.90\delta$ for mildly

relativistic electrons. It decreases to $\alpha = 0.5(1 - \delta)$ for relativistic electrons.

Nita et al. (2004) reported a trend that the microwave spectra both above and below the peak frequency become flatter with increasing peak flux. The evolution of the high-frequency spectrum is easily understood, because more high-energy electrons means higher brightness. Since the flattening of the low-frequency spectrum translates non-uniformities in the radio sources, the observed trend of the low-frequency spectrum probably means that the more intense microwave bursts are emitted by more complex sources.

2.4. Analysis of electron spectra from microwave and HXR observations

There has been a long-standing discussion in the literature on the discrepancy of energy spectra of the radiating electrons derived from HXR and microwave spectral observations. While early analyses came to the overall conclusion that the HXR emission required many more non-thermal electrons than the microwaves, more sophisticated later models, which considered differences between the HXR source (thick target or trap-plus-precipitation) and the microwave sources and also the possibility of absorption or suppression and of inhomogeneous magnetic fields of the microwave emission mostly concluded that the electron populations were compatible (see Pick et al., 1990, and references therein). This does not exclude the possibility that different parts of a common electron spectrum emit the two wavelength ranges, since HXR are mostly emitted by electrons of lower energy than microwaves.

Pioneering observations of microwave emission in the mm-waveband were discussed by Kundu et al. (1994). While the hard X-ray bursts they studied had particularly steep spectra (indices >6), so that no high-frequency microwave emission was expected, the BIMA interferometer did see emission at 86 GHz which the authors ascribed to electrons with a much flatter power law energy spectrum. Since these flares had no detectable γ -ray continuum from the high-energy electrons presumed to emit the mm-waves, a consistency check between the two spectral domains could not be made. Such complementary studies were carried out through the comparison of microwave and gamma-ray spectra during two large flares by Trotter et al. (1998, 2000). During these events the photon spectrum derived from the HXR and γ -rays hardened above a break in the range (400–700) keV. This was interpreted as a hardening of the high-energy electron spectrum. Depending on whether the optically thin microwave emission comes from the electrons below or above the break, the microwave spectral index should be compatible with the electron spectral index

inferred from hard X-rays or γ -rays, respectively. Hildebrandt et al. (1998) showed that for typical magnetic fields and break energies in the range (100–500) keV the microwave spectrum will have a break in the range (10–30) GHz.

Trotter et al. (1998, 2000) found that the electron spectral index derived from observations at frequencies between 20 and 50 GHz was consistent with the γ -rays. This finding confirms the view that microwave emission at short cm-waves and mm-waves comes from relativistic electrons, and that these electrons may have a flatter spectrum than the electrons up to a few hundreds of keV which dominate the HXR photon spectrum. This is so although the time profile of the microwave emission resembles that of the HXR – a similarity which had been used as an argument that the microwaves are emitted by the same electron populations as the HXR at some tens to a few hundreds of keV (Kosugi et al., 1988).

The analysis of the γ -ray flare of 2002 July 23 observed by RHESSI and NoRH was interpreted by White et al. (2003) as a counterexample to this conclusion. The event was very bright and optically thick up to the vicinity of 35 GHz. From measurements at 35 and 80 GHz, the authors derived a spectral index of the electrons that gradually rises from -3.3 to -2.4 during the phase of bright emission (see Fig. 1 of White et al., 2003). The spectral index will be steeper if 35 GHz is not in the optically thin regime. The HXR/ γ -ray continuum was fitted by a spectrum with slope 2.77 (2.23) at energies below (above) about 600 keV (Smith et al., 2003). Assuming a thick target model, this photon spectrum implies an electron number spectrum with slope 4.3 (3.2), where electrons emitting photons above 600 keV were supposed to travel at c . The value derived from the high-energy photons is not far from the value inferred from the microwaves. Contribution of electron–electron bremsstrahlung to the γ -ray continuum emission would imply a slightly steeper electron spectrum (see Haug, 1975), and would hence produce a discrepancy with the microwaves. But in the light of the observational uncertainties the 2002 July 23 flare does not appear as a clear contradiction to the conclusion from the large flares mentioned above: that electron spectra inferred from high-frequency microwave and γ -ray continuum observations are compatible, whilst the electrons with lower energies emitting hard X-rays up to a few hundreds of keV may have steeper spectra.

With the data presently at hand, the modelling must assume simple configurations, e.g., homogeneous energy spectra (although the magnetic field model may be non-uniform) and isotropic angular distributions of the non-thermal electrons. There is some degree of freedom because the electrons emitting microwaves may be trapped, while precipitating electrons are often assumed for hard X-rays. While the events analysed by

Trottet et al. (1998, 2000) and White et al. (2003) suggest that the electrons emitting mm-waves are not efficiently trapped, the model calculations of another event by Bruggmann et al. (1994) showed a good correspondence with the observed time profiles and spectra of HXR and microwaves under the assumption that both are produced by electrons injected during several minutes into a coronal trap. The trapping was suggested in this case by large delays (several tens of seconds) between the peaks at microwaves, high-energy and low-energy hard X-rays. Such delays do not exist in the events discussed above, so that the electron dynamics seems to be different in these events. However, Bruggmann et al. (1994) had no γ -ray continuum measurements able to provide an independent diagnostic of the relativistic electron spectrum. In summary, the model calculations seem to converge to the idea that microwaves and γ -rays, potentially also hard X-rays, give a consistent view of the spectrum of radiating electrons, but that this spectrum is not necessarily a unique power-law, and that furthermore there is a great amount of inherent uncertainty due to a simplified view of electron transport imposed by the presently available data.

2.5. *An open issue: angular distributions of the radiating electrons*

It may appear surprising that such simple models of the electron distribution as usually employed in HXR and microwave analyses lead to relevant results at all, because anisotropies of the angular distributions are expected to have a strong influence on the intensity and the spectral slope of gyrosynchrotron emission (Ramaty, 1969; Fleishman and Melnikov, 2003). The spectrum and intensity of gyrosynchrotron emission depend on the viewing angle with respect to the magnetic field and to the pitch angle of the radiating electrons. Relativistic beaming favours strong emission in the instantaneous direction of motion, while the Lorentz force tends to favour strong emission in the direction perpendicular to the magnetic field. Nevertheless, effects of anisotropy expected in homogeneous models like cutoffs of the high-frequency spectrum are not apparent in the data. Although mm-wave observations are still scarce, observations up to 86 GHz (Raulin et al., 1999) and even above 200 GHz (Trottet et al., 2002; Lüthi et al., 2004) seem to suggest that the gyrosynchrotron spectrum continues up to high frequencies. It is important to keep in mind that such microwave spectra are flux density spectra without spatial resolution. High-frequency emission from regions of strong magnetic fields (cf. de Jager et al., 1987; Klein, 1987) may then compensate for the absence of optically thin emission from weaker fields, and mimic a continuous power law decrease of the high-frequency spectrum although different sources are actually involved. Spectroscopic imaging

over an extended range of microwave frequencies is needed to give us a clearer view.

Possible observational evidence for anisotropies of the electron distribution at microwaves was presented by Melnikov et al. (2002) and White et al. (2002). They showed several NoRH observations of flares, where the microwave emission comes initially from loop footpoints as expected from optically thin gyrosynchrotron emission, but later on a single source near the summit of the former loop dominates, although the emission remains optically thin. The authors ascribe the late emission to loop top sources, and suggest they were emitted by trapped electrons. Model computations by Melnikov et al. (2002) show that an electron distribution peaked perpendicular to the magnetic field around the summit would reproduce the observations. While the interpretation of these optically thin loop-top sources in terms of anisotropic distribution functions is promising, spatial structure of the radio sources on unresolved scales may be an alternative. The simple events discussed in Sections 2.1 and 2.2 suggest that the sources may be as small as the 10'' resolution of NoRH or even smaller. The brightening of such a compact source below an extended one would mimic a loop top source. Spectral imaging with higher spectral and spatial resolution is required to disentangle these effects. It is clear that the unsolved issue on the angular distribution of the radiating electrons is a major obstacle to more refined quantitative interpretations of the observations.

2.6. *Can microwave and HXR emission provide evidence on the accelerated electron population?*

All the discussions of the present section rely on the assumption that the observed spatial and spectral features of the microwave emission reveal properties of the distributions of energies and pitch angles of the radiating electrons. However, if the relevant electron dynamics occur in a multitude of small-scale regions which are not resolved by imaging observations, any modelling effort as those cited above will stand on uncertain ground, and the quantitative results from such efforts will be of questionable significance. As interesting as it may appear on theoretical grounds (cf. Vlahos et al., 2004, and references therein), this objection seems to exclude the possibility of correlated behaviour of electron signatures in different flaring regions, such as the correlated brightenings of different HXR footpoints (Sakao et al., 1994), correlated variations of coherent radio and HXR emission (Aschwanden, 2002, and references therein) or of different microwave sources (Hanaoka, 1999). The existence of correlations suggests that we do see at least some features related to electron transport, although elementary acceleration processes occur on subtelesopic scales. Similarly, the understanding of the global features of microwave and HXR source

morphology in terms of gyrosynchrotron radiation and bremsstrahlung, outlined in previous sections, suggests that the available observations can be related to microscopic processes.

3. Radio observations of energy release and acceleration sites

3.1. Evidence from electron beams

The centimetric imaging observations discussed above suggest that interacting loops in the low corona provide a site for electron acceleration to hundreds of keV. There is no hint in this data to cases with loop top sources as were found in HXR, since the loop top sources of White et al. (2002) and Melnikov et al. (2002) occur in the course of a flare, rather than at its beginning.

Independent evidence on electron acceleration sites in the corona comes from broadband spectrographic observations. Coherent emission at long centimetric-to-metric wavelengths comprises short bursts emitted by electron beams at the local plasma frequency or its harmonic. The bursts exhibit a characteristic frequency drift to higher or lower frequencies, depending on whether the beams travel along the gradient of ambient electron density or in the opposite direction. Bursts drifting to lower frequencies are called type III bursts, those drifting to higher frequencies reverse-drift bursts (RS bursts). Aschwanden et al. (1995) studied correlated decimetric-to-metric type III bursts and individual peaks in the HXR time profile. The existence of such a correlation points to the generation of bidirectional electron beams in the corona, the upward propagating beams being revealed by type III emission, whereas the downward propagating beams generate HXR in the dense low atmosphere. In some cases downward propagating beams are also signalled by RS bursts. The starting frequencies of the type III bursts between 220 and 910 MHz imply a range of thermal electron densities in the acceleration region $(6 - 100) \times 10^8$ $((1.5 - 26) \times 10^8)$ cm^{-3} for fundamental (harmonic) emission (Aschwanden and Benz, 1997). The start frequencies of successive bursts in the course of an event scatter within a frequency range (20%–50%) of the central frequency (Aschwanden, 2002). He suggests that the gap between the start of oppositely drifting bursts characterises individual acceleration regions (typical size 100–1000 km), while the overall scatter characterises the volume where accelerators exist (5000–50000 km).

A key result of Aschwanden and Benz (1997) is the much lower electron density in the acceleration region than in the bright soft X-ray loops ($n_e = (0.2 - 2.5) \times 10^{11} \text{ cm}^{-3}$). The authors explain this by acceleration regions outside the bright SXR loops, e.g., reconnection in

a cusp geometry above the loops. This is consistent with electron time-of-flight studies from HXR (Aschwanden, 2002) as well as with geometries inferred for HXR loop top sources. But the relative timing of the electron acceleration and the filling of the loops is not clear, since the high electron densities in flaring X-ray loops are generally ascribed to chromospheric evaporation, which the Neupert effect (Neupert, 1968; Dennis and Zarro, 1993) links closely to the acceleration of HXR or microwave-emitting electrons. This scenario is corroborated by correlative radio and HXR observations not only with soft X-rays, but also EUV and H α (Trottet et al., 2000, and references therein). One should therefore not expect that such dense loops already exist when the electrons carrying the bulk of the released energy start to be accelerated.

The typical height where electrons of tens to a few hundreds of keV are accelerated are estimated from time-of-flight analyses as 1.4 times the loop radius seen in soft X-rays (cf. Aschwanden, 2002 and references therein). The cusp geometry envisaged by Aschwanden and Benz (1997) is shown in Fig. 4, and compared with that inferred for the acceleration of electrons of several hundreds of keV from the NoRH microwave imaging (Hanaoka, 1999). The inferred heights of the acceleration regions are comparable, although the details of the scenarios show differences. For instance, microwave emission from the very dense soft X-ray loops in Fig. 4(a) may be suppressed by the Razin effect. Simple estimates based on the densities and temperatures derived from the soft X-rays (Aschwanden and Benz, 1997) do show that Razin suppression could act up to several tens of GHz. The microwave spectrum of such a source would be limited to very high frequencies. Spectra with a possible influence of Razin suppression were discussed in the literature (Kaufmann et al., 1985; Klein, 1987; Belkora, 1997), but not in conjunction with the soft X-ray and type III burst diagnostics of Aschwanden and Benz (1997). The available spatial resolution does not allow one to distinguish between microwave emission in the sources “SXR” and “MW” in Fig. 4(a). Radio imaging observations that encompass the centimetric-to-metric waveband, and their combination with knowledge of the magnetic field structure in X-ray and radio emitting regions, are required to conceive a coherent scenario of interacting and escaping particles, and of the different energy ranges of energetic electrons.

3.2. Decimetric spikes

The basic idea that electron acceleration in the corona can be traced by short-lived and narrow-banded radio emission (spikes) is corroborated by spectral and imaging observations at metre waves (Krucker et al., 1997; Paesold et al., 2001, and references therein). Metric spikes are observed near the starting frequency of type

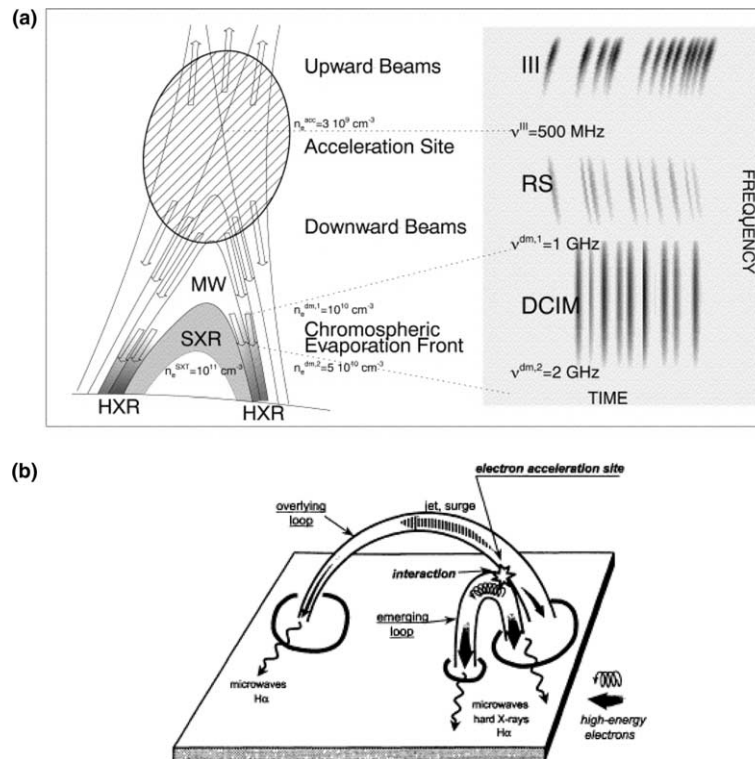


Fig. 4. Scenarios of the acceleration of electrons of tens of keV inferred from soft X-ray and radio spectroscopic observations (a; [Aschwanden and Benz, 1997](#)) and of electrons of several hundreds of keV as inferred from microwave imaging (b; [Hanaoka, 1999](#)).

III bursts, and their sources are located in the backward extrapolation of the type III trajectories. The studied events occur at greater coronal altitudes than inferred for the acceleration of electrons during flares. They are related with electron beams escaping to the high corona (metric type III bursts) outside flares, since there is no HXR or microwave emission.

The HXR associated decimetric spikes have only rarely been mapped, and their location with respect to HXR and microwave signatures of energetic electrons is basically unexplored. [Benz et al. \(2002\)](#) studied events where the low-frequency part of spike clusters could be located by the Nançay Radioheliograph. They found the spike sources far from the hard X-ray sources, but the morphology of the magnetic structures was complicated in their events. Since spikes are due to coherent emission processes, it is expected that their overall spectral extent reflects distributed regions of acceleration. One may speculate that the lower outskirts of the acceleration region from which spikes at relatively low frequencies are seen are not the regions where the most energetic electrons are accelerated. Again, the lack of imaging observations over the whole frequency range where spikes occur sets limits to our ability of exploring acceleration sites. Only when the low-frequency part and the high-frequency part of the clusters will be imaged and compared with magnetic field extrapolations will we be able to give a clearer statement on the relevance of decimetric spikes as tracers of electron acceleration during flares.

Doubts on such a central role come from the delays of spikes after HXR emission, up to several seconds ([Aschwanden and Guedel, 1992](#)). It is not clear if such delays can be explained by coronal transport, since the earlier HXR emission clearly shows that electrons are precipitated in the low atmosphere up to several seconds before the first spikes are observed in the dynamic spectra. Alternatively, the spikes might also be related with electron transport to the remote microwave source discussed in Section 2.2. The delays of spikes are much longer than those observed from microwaves ([Hanaoka, 1999](#)), but this may be due to the different energy ranges of the radiating electrons, i.e., tens of keV for the spikes, hundreds of keV for the microwaves.

3.3. Possible radio signatures from regions of magnetic reconnection

Spectroscopic studies provided other, less indirect signatures which may be related to the energy release and electron acceleration during solar flares.

[Kliem et al. \(2000\)](#) studied the time evolution of the radio spectrum during a burst related with a “plasmoid ejection” observed in soft X-rays (Yohkoh/SXT). The radio emission exhibited quasi-periodic pulsations whose envelope gradually drifted to lower frequencies. Using an MHD model of dynamic magnetic reconnection in a large scale current sheet above the top of coronal loops, [Kliem et al.](#) showed that magnetic islands

form and coalesce repeatedly and gradually build up a large-scale plasmoid that is accelerated outward. Electrons are quasi-periodically accelerated during the formation of the magnetic islands. Their increasing height explains the gradual drift of the radio emission towards lower frequencies.

Electron acceleration at the shock of a reconnection outflow was argued by Aurass et al. (2002) and Aurass and Mann (2004) to be at the origin of a specific radio spectral signature which in many respects resembles type II emission from travelling shocks in the corona, e.g., through the presence of both fundamental and harmonic emission or of splitted bands of emission. But unlike type II emission the new signature displays little or no frequency drift, which led the authors to ascribe it to a standing shock generated by the downward propagating jet from a coronal reconnection region. This type of emission was found in the late impulsive as well as during the extended phase of flares, coming from sources above soft X-ray loops. The complexity of the radio spectra during large bursts makes it likely that the signature is easily hidden during impulsive flare phases, and could be much more frequent than the definite detections suggest.

A further spectral signature recently discovered are sawtooth-shaped oscillations (Klassen et al., 2001), which were also interpreted as signatures of energy release, in analogy with observations in tokamaks (see also discussion in Kliem et al., 2003).

4. Conclusion

Radio waves provide a variety of diagnostics on electron acceleration during solar flares. We owe to microwave imaging and modelling information on the mildly relativistic part of the electron populations accelerated during flares which are not accessible to present sensitivities of HXR or γ -ray imagers. That mildly relativistic electrons are the emitters of cm- and mm-wavelength emission has been confirmed by recent joint studies in a few cases where γ -ray continua could be measured. Decimetric spectroscopy has shown an increasing number of signatures that can be related to the acceleration processes, although much of the interpretation is speculative for the time being. A lacking element for further understanding is imaging observations which, although the sources emitting spectral fine structure cannot be resolved, would allow one to localise them with respect to the global magnetic field configuration.

From this, two new tools of investigation will be needed in the future: the extension to higher frequencies and spectral imaging over the whole range from millimetre to metre waves. Observations with BIMA and now the *Solar Submillimeter Telescope* (Kaufmann et al., 2001; Gimenez de Castro et al., 2005) and the *Köln*

Observatory for Submillimeter and Millimeter Astronomy (KOSMA; Lüthi et al., 2004) and their possible extensions to shorter wavelengths promise to be a unique tool to probe up to which energies electrons can be accelerated during solar flares, and thereby to constrain the potential acceleration mechanisms. An open task is the connection of the various pieces of information from different ranges of the radio spectrum that have been discussed here, from microwaves to metre wavelengths. The *Frequency Agile Solar Radio Telescope* project (FASR, Bastian, 2003) is the promising tool to achieve this performance.

Acknowledgements

The author acknowledges G. Hurford and N. Vilmer for organising the session on High Energy Processes at the 35th COSPAR assembly, G. Trotter, and S. White for helpful discussions especially on the interpretation of X-ray and microwave spectra, and A. MacKinnon and E. Kontar for advice on electron–electron bremsstrahlung. The referees are thanked for helpful suggestions.

References

- Alissandrakis, C.E., Preka-Papadema, P. Microwave emission and polarization of a flaring loop. *A&A* 139, 507–511, 1984.
- Aschwanden, M.J. Particle acceleration and kinematics in solar flares. *Space Sci. Rev.* 101, 1–227, 2002.
- Aschwanden, M.J., Benz, A.O. Electron densities in solar flare loops, chromospheric evaporation upflows, and acceleration sites. *ApJ* 480, 825–839, 1997.
- Aschwanden, M.J., Guedel, M. The coevolution of decimetric millisecond spikes and hard X-ray emission during solar flares. *ApJ* 401, 736–753, 1992.
- Aschwanden, M.J., Benz, A.O., Dennis, B.R., Schwartz, R.A. Solar electron beams detected in hard X-rays and radio waves. *ApJ* 455, 347–365, 1995.
- Aurass, H., Mann, G. Radio observation of electron acceleration at solar flare reconnection outflow termination shocks. *ApJ* 615, 526–530, 2004.
- Aurass, H., Vršnak, B., Mann, G. Shock-excited radio burst from reconnection outflow jet?. *A&A* 384, 273–281, 2002.
- Bastian, T.S. The frequency agile solar radiotelescope. *Adv. Space Res.* 32, 2705–2714, 2003.
- Bastian, T.S., Benz, A.O., Gary, D.E. Radio emission from solar flares. *Ann. Rev. Astron. Astrophys.* 36, 131–188, 1998.
- Belkora, L. Time evolution of solar microwave bursts. *ApJ* 481, 532–544, 1997.
- Benka, S.G., Holman, G.D. A thermal/nonthermal model of solar microwave bursts. *ApJ* 391, 854–864, 1992.
- Benz, A.O., Saint-Hilaire, P., Vilmer, N. Location of narrowband spikes in solar flares. *A&A* 383, 678–684, 2002.
- Bruggmann, G., Vilmer, N., Klein, K.-L., Kane, S.R. Electron trapping in evolving coronal structures during a large gradual hard X-ray/radio burst. *Solar Phys.* 149, 171–193, 1994.
- Correia, E., Kaufmann, P., Magun, A. The observed spectrum of solar burst continuum emission in the submillimeter spectral range. In:

- Rabin, D.M., Jefferies, J.T., Lindsey, C. (Eds.), IAU Symposium 154: Infrared Solar Physics. Kluwer, Dordrecht, pp. 125–129.
- de Jager, C., Kuipers, J., Correia, E., Kaufmann, P. A high-energy solar flare burst complex and the physical properties of its source region. *Solar Phys.* 110, 317–326, 1987.
- Dennis, B.R., Zarro, D.M. The Neupert effect – What can it tell us about the impulsive and gradual phases of solar flares?. *Solar Phys.* 146, 177–190, 1993.
- Dulk, G.A. Radio emission from the sun and stars. *Ann. Rev. Astron. Astrophys.* 23, 169–224, 1985.
- Dulk, G.A., Marsh, K.A. Simplified expressions for the gyrosynchrotron radiation from mildly relativistic, nonthermal and thermal electrons. *ApJ* 259, 350–358, 1982.
- Fleishman, G.D., Melnikov, V.F. Gyrosynchrotron emission from anisotropic electron distributions. *ApJ* 587, 823–835, 2003.
- Gimenez de Castro, C.G., Kaufmann, P., Raulin, J.-P. Recent results of solar activity diagnostics at submillimeter wavelengths. *Adv. Space Res.* 2005, this issue.
- Guidice, D.A., Castelli, J.P. Spectral distributions of microwave bursts. *Solar Phys.* 44, 155–172, 1975.
- Hanaoka, Y. Double-loop configuration of solar flares. *Solar Phys.* 173, 319–346, 1997.
- Hanaoka, Y. High-energy electrons in double-loop flares. *PASJ* 51, 483–496, 1999.
- Haug, E. Contribution of electron–electron bremsstrahlung to solar hard X-radiation during flares. *Solar Phys.* 45, 453–458, 1975.
- Hildebrandt, J., Krüger, A., Chertok, I.M., Fomichev, V.V., Gorgutsa, R.V. Solar microwave bursts from electron populations with a ‘broken’ energy spectrum. *Solar Phys.* 181, 337–349, 1998.
- Kai, K. Microwave sources of solar flares – loop top or foot points?. *Solar Phys.* 111, 81–87, 1987.
- Kaufmann, P., Correia, E., Costa, J.E.R., Vaz, A.M.Z., Dennis, B.R. Solar burst with millimetre-wave emission at high frequency only. *Nature* 313, 380–382, 1985.
- Kaufmann, P., Raulin, J.-P., Correia, E., Costa, J.E.R., Guillermo, C., de Castro, G., Silva, A.V.R., Levato, H., Rovira, M., Mandrini, C., Fernández-Borda, R., Bauer, O. Solar flare observations at submm-waves. In: Brekke, P., Fleck, B., Gurman, J.B. (Eds.), IAU Symposium 203: Recent Insights into the Physics of the Sun and Heliosphere: Highlights from SOHO and Other Space Missions. *Astron. Soc. Pac.*, p. 283, 2001.
- Klassen, A., Aurass, H., Mann, G. Sawtooth oscillations in solar flare radio emission. *A&A* 370, L41–L44, 2001.
- Klein, K.-L. Microwave radiation from a dense magneto-active plasma. *A&A* 183, 341–350, 1987.
- Klein, K.-L., Trottet, G. Gyrosynchrotron radiation from a source with spatially varying field and density. *A&A* 141, 67–76, 1984.
- Kliem, B., Karlický, M., Benz, A.O. Solar flare radio pulsations as a signature of dynamic magnetic reconnection. *A&A* 360, 715–728, 2000.
- Kliem, B., MacKinnon, A., Trottet, G., Bastian, T.S. Recent progress in understanding energy conversion and particle acceleration in the solar corona. In: Klein, K.-L. (Ed.), *Energy Conversion and Particle Acceleration in the Solar Corona*, Lecture Notes in Physics, vol. 612. Springer, Berlin, pp. 263–293, 2003.
- Kosugi, T., Dennis, B.R., Kai, K. Energetic electrons in impulsive and extended solar flares as deduced from flux correlations between hard X-rays and microwaves. *ApJ* 324, 1118–1131, 1988.
- Krucker, S., Benz, A.O., Aschwanden, M.J. YOHKOH observation of the source regions of solar narrowband, millisecond spike events. *A&A* 317, 569–579, 1997.
- Kundu, M.R., White, S.M., Gopalswamy, N., Lim, J. Millimeter, microwave, hard X-ray, and soft X-ray observations of energetic electron populations in solar flares. *ApJ Suppl.* 90, 599–610, 1994.
- Kundu, M.R., White, S.M., Shibasaki, K., Sakurai, T., Grechnev, V.V. Spatial structure of simple spiky bursts at microwave/millimeter wavelengths. *ApJ* 547, 1090–1099, 2001.
- Lüthi, T., Magun, A., Miller, M. First observation of a solar X-class flare in the submillimeter range with KOSMA. *A&A* 415, 1123–1132, 2004.
- Melnikov, V.F., Shibasaki, K., Reznikova, V.E. Loop-top nonthermal microwave source in extended solar flaring loops. *ApJ* 580, L185–L188, 2002.
- Neupert, W.M. Comparison of solar X-ray line emission with microwave emission during flares. *ApJ* 153, L59–L64, 1968.
- Nindos, A., White, S.M., Kundu, M.R., Gary, D.E. Observations and models of a flaring loop. *ApJ* 533, 1053–1062, 2000.
- Nishio, M., Yaji, K., Kosugi, T., Nakajima, H., Sakurai, T. Magnetic field configuration in impulsive solar flares inferred from coaligned microwave/X-ray images. *ApJ* 489, 976–991, 1997.
- Nita, G.M., Gary, D.E., Lee, J. Statistical study of two years of solar flare radio spectra obtained with the Owens Valley Solar Array. *ApJ* 605, 528–545, 2004.
- Paesold, G., Benz, A.O., Klein, K.-L., Vilmer, N. Spatial analysis of solar type III events associated with narrow band spikes at metric wavelengths. *A&A* 371, 333–342, 2001.
- Pick, M., Klein, K.-L., Trottet, G. Meter-decimeter and microwave observations of solar flares. *ApJ Suppl.* 73, 165–175, 1990.
- Preka-Papadema, P., Alissandrakis, C.E. Spatial and spectral structure of a solar flaring loop at centimeter wavelengths. *A&A* 191, 365–373, 1988.
- Preka-Papadema, P., Alissandrakis, C.E. Two-dimensional model maps of flaring loops at cm-wavelengths. *A&A* 257, 307–314, 1992.
- Ramaty, R. Gyrosynchrotron emission and absorption in a magneto-active plasma. *ApJ* 158, 753–769, 1969.
- Raulin, J.P., White, S., Kundu, M., Silva, A., Shibasaki, K. Multiple components in the millimeter emission of a solar flare. *ApJ* 522, 547–558, 1999.
- Sakao, T., Kosugi, T., Masuda, S., Yaji, K., Inada-Koide, M., Makishima, K. Hard X-ray imaging observations of footpoint sources in impulsive solar flares. In: Enome, S., Hirayama, T. (Eds.), *Proceedings of Kofu Symposium*. NRO Report 360, Nobeyama, pp. 169–172, 1994.
- Smith, D.M., Share, G.H., Murphy, R.J., Schwartz, R.A., Shih, A.Y., Lin, R.P. High-resolution spectroscopy of gamma-ray lines from the X-class solar flare of 2002 July 23. *ApJ* 595, L81–L84, 2003.
- Trottet, G., Raulin, J., Kaufmann, P., Siarkowsky, M., Klein, K.-L., Gary, D. First detection of the impulsive and extended phases of a solar radio burst above 200 GHz. *A&A* 381, 694–792, 2002.
- Trottet, G., Rolli, E., Magun, A., Barat, C., Kuznetsov, A., Sunyaev, R., Terekhov, O. The fast and slow Hz chromospheric responses to non-thermal particles produced during the 1991 March 13 hard X-ray/gamma-ray flare at ~08 UTC. *A&A* 356, 1067–1075, 2000.
- Trottet, G., Vilmer, N., Barat, C., Benz, A., Magun, A., Kuznetsov, A., Sunyaev, R., Terekhov, O. A multiwavelength analysis of an electron-dominated gamma-ray event associated with a disk solar flare. *A&A* 334, 1099–1111, 1998.
- Vilmer, N., MacKinnon, A. What can be learned about competing acceleration models from multiwavelength observations?. In: Klein, K.-L. (Ed.), *Energy Conversion and Particle Acceleration in the Solar Corona*, Lecture Notes in Physics, vol. 612. Springer, Berlin, pp. 127–160, 2003.
- Vlahos, L., Isliker, H., Lepreti, F. Particle acceleration in an evolving network of unstable current sheets. *ApJ* 608, 540–553, 2004.
- White, S.M., Kundu, M.R., Garaimov, V.I., Yokoyama, T., Sato, J. The physical properties of a flaring loop. *ApJ* 576, 505–518, 2002.
- White, S.M., Krucker, S., Shibasaki, K., Yokoyama, T., Shimojo, M., Kundu, M.R. Radio and hard X-ray images of high-energy electrons in an X-class solar flare. *ApJ* 595, L111–L114, 2003.
- Yokoyama, T., Nakajima, H., Shibasaki, K., Melnikov, V.F., Stepanov, A.V. Microwave observations of the rapid propagation of nonthermal sources in a solar flare by the Nobeyama Radioheliograph. *ApJ* 576, L87–L90, 2002.